

# INTERFERENCE ANALYSIS IN THE MULTI-SERVICE UNIVERSAL FILTERED MULTICARRIER SYSTEMS

**RAJARAO MANDA,**

PhD and Assistant Professor, Dept. of Electrical and Electronics Engineering, School of Engineering, UPES, Dehradun, India.

**R GOWRI**

Professor, Dept. of Electrical and Electronics, School of Engineering, UPES, Dehradun, India.

## Abstract

The Universal Filtered Multicarrier (UFMC) is an emerging modulation waveform technique for next-generation wireless networks. The sub-band filtering operation may disrupt the orthogonality between the subcarriers, which causes inter-carrier interference (ICI) and inter sub-band interference (ISBI) (i.e., the quantity of interference on the neighboring sub-bands) and degrades the system performance. Thus, the sub-band filter design in UFMC based systems plays an important role in its performance. This paper analyzes the interference in the multi-service/user-based UFMC system with the closed-form of the interference variance in terms of sub-band size and filter length. In addition, the sub-band filter configuration is adapted according to the sub-band size (i.e., number of subcarriers per sub-band) such that the system generates the minimum level of interference. With the proposed method, the overall signal to interference ratio improved by around 8 dB. Further, the transmission time interval (TTI) of the UFMC symbol could be reduced by shortening the symbol overhead (filter tail) and hence improving the frame efficiency.

**Keywords:** Fifth Generation (5G), 5G waveform, Finite Impulse Response (FIR) filter, Inter Carrier Interference (ICI), Inter Sub-band Interference (ISBI), maximum-to-minimum filter gain ratio, Signal to Interference Ratio (SIR), Universal Filtered Multi-Carrier (UFMC).

## INTRODUCTION

In recent years, the fast growth of smart terminals, real-time interactive services, and the internet of everything (IoE) motivated the 5G evolution (i.e., 6G wireless networks). The requirements of the new generation of the cellular network define the following goals: to enhance broadband connectivity, to reduce energy consumption and reduce latency for ultra-reliable low latency communication, and to achieve intelligent communication [1]–[3]. Orthogonal frequency division multiplexing (OFDM) was one of the most widely adopted modulation waveforms in the present broadband wireless systems [4]. However, some of the weaknesses of OFDM which include large side lobes, bandwidth utilization, high peak to average power ratio, and severe synchronization requirements made it inadequate for 5G and beyond 5G wireless systems. These limitations enforce the design of a new and flexible modulation waveform that needs to support asynchronous transmission, lower out of band emission (OBE), and lower latency with less baseband system complexity [5]–[7]. In the last few years, several waveform candidates such as generalized frequency-division multiplexing (GFDM) [8], filter bank multicarrier (FBMC) [9], filtered orthogonal frequency-division multiplexing (F-OFDM) [10], and universal filtered multicarrier (UFMC) [11] have been proposed for next-generation wireless communication systems with a lower OBE. Among them, the UFMC waveform is the most recommended candidate waveform in the 5G and beyond 5G wireless systems to

meet the main key performance parameters such as lower OBE, flexible packet transmission, and relaxed synchronization with low latency and system flexibility [12]–[14].

The UFMC waveform is a combined form of FBMC and F-OFDM, in which, a group of subcarriers (SCs) is filtered individually. The filtering operation in UFMC makes it more robust in relaxed synchronization conditions compared to OFDM, reduces the out-of-band emission (OBE), and is highly suitable for short packet transmission. The sub-band filtering can be physical resource block (PRB) based, service-based, and user-based [15], [16]. The UFMC is suitable for PRB based sub-band filtering and massive machine-type communications and the F-OFDM may favor user- or service-based sub-band filtering for enhanced mobile broadband. The main drawback of the F-OFDM waveform uses a longer filter length than the UFMC waveform which is half of the OFDM symbol and which increases the latency. The multi-service or multi-user approach may save the signaling overhead but the sub-band filtering disrupts the orthogonality between the sub-carriers and introduces inter-carrier interference (ICI) and inter-sub band/service interference (ISBI). In addition, the baseband complexity and computation complexity of the UFMC system are higher than the conventional OFDM due to the number of IFFT blocks and sub-band filters.

Recently, there are several filter optimization and baseband signal processing approaches have been proposed to mitigate the interference in the UFMC system [17]–[21]. The sub-band FIR filter is optimized based on the knowledge of expected timing offset and frequency offset to reduce the out-band radiation [17], [18] and hence reduced the interference between the adjacent sub-bands. The active interference cancellation approach suggested in [19] uses a separate subcarrier inserted on both sides of the sub-band for interference cancellation and optimizes the weights of these subcarriers to maximize the overall signal-to-interference noise ratio (SINR) under the power constraints. With this approach, the spectral efficiency degraded due to the use of separate subcarriers for interference cancellation. An adaptive modulation and filter configuration was proposed in [20], in which the sub-band filter impulse response parameters were determined adaptively to reduce the interference caused by carrier frequency offset (CFO).

For the UFMC system, the sub-band filter operation protects from multipath fading effect and inter-symbol interference (ISI) like a cyclic prefix (CP) in the OFDM system. However, the ramp (filter tail) of the sub-band filter on both sides of the symbol causes interference on the neighbor sub-bands, which relies upon the filter length. In practice, the sub-band filter length is preferred longer or equal to the wireless channel length to avoid the multipath fading effect [11]. In some scenarios, the short filter length can be sufficient to get marginal system performance, which means further the system overhead can be reduced reasonably. In this paper, we derived the closed form for the interference in the UFMC symbol due to filtering operation and then optimize the filter length with respect to sub-band size. Here the sub-carrier (sub-band size) allocation to each user depends on the user or service request such as data, video streaming, or online interactive game services. So, the length of each sub-band is different from the other. Which makes fewer computations at the sub-band filter and improves the symbol utilization ratio.

The remaining part of the paper is as follows: Section 2 carries the discussion of the multi-user UFMC transmitter model. Section 3 focuses on the analysis of ISBI and ICI variation with respect to filter length and sub-band size, and includes the computation of filter parameters for 5G-NR numerology. Section 4 discusses the simulation result, and performance comparison of the UFMC system, and finally, Section-5 concludes this paper.

## 2 THE UFMC WAVEFORM MODEL

Figure 1 shows the functional block diagram of the UFMC system model. On the side of the UFMC transmitter, the total number of data subcarriers  $N_{DC}$  (bandwidth) is divided into a group of consecutive subcarriers (known as sub-band) and a specific constellation modulated (Quadrature Amplitude Modulation (QAM)) data samples allocated to each sub-band. After performing the subcarrier mapping on a total number of subcarriers ( $N$ ) and zeros padded to the unallocated subcarriers, each sub-band is processed through  $N$ -point IFFT. These time-domain sub-band signals are filtered individually with an FIR filter and summed to generate the UFMC signal. In the case of a multi-service/user-based communication system, multiple PRBs allocated to each user or service are considered sub-band. Let consider  $B$  number of sub-bands and each sub-band carries  $Q_p$  number of subcarriers i.e.,  $\sum_{p=0}^{B-1} Q_p = N_{DC}; p = 0, 1, \dots, B - 1$ . The final UFMC signal has a length of  $N + L_f - 1$  can be expressed as

$$x(n) = \sum_{p=0}^{B-1} x_p(n) = \sum_{p=0}^{B-1} \sum_{l=0}^{L_f-1} f_p(l) s_p(n-l) \quad (1)$$

Where  $n = 0, 1, 2, \dots, N + L_f - 2$  and  $L_f$  is the sub-band FIR filter length,  $f_p(l)$  represents the filter impulse response of  $p^{\text{th}}$  sub-band, which is the center frequency shifted of the prototype filter impulse response ( $f(l)$ ) corresponding to the sub-band. That is,

$$f_p(l) = f(l) e^{j \frac{2\pi}{N} (K_0 + K_{pshift}) l}; l = 0, 1, \dots, L_f - 1 \quad (2)$$

Where  $K_{pshift} = \sum_{b=0}^{p-1} Q_b + Q_p/2$ ;  $K_0 = \frac{N - N_{DC}}{2}$  denotes the starting subcarrier index of the lowest sub-band of the UFMC signal. The time-domain signal  $s_p(n)$  represents the  $N$ -point IFFT of  $p^{\text{th}}$  sub-band written as

$$s_p(n) = \frac{1}{N} \sum_{k=0}^{Q_p-1} S_p(k) e^{j \frac{2\pi}{N} (K_0 + K_p + k) n}; n = 0, 1, \dots, N - 1 \quad (3)$$

Where the sequence  $S_p(k)$  represents the  $p^{\text{th}}$  sub-band data samples and  $K_p = \sum_{b=0}^{p-1} Q_b$ . The transmitted UFMC signal can write in matrix form as

$$X = \sum_{p=0}^{B-1} [F_p]_{(N+L_f-1) \times N} [V_p]_{N \times Q_p} [S_p]_{Q_p \times 1} \quad (4)$$

where  $[F_p]_{(N+L_f-1) \times N}$  is a Toeplitz matrix of  $p^{\text{th}}$  sub-band FIR filter impulse response with the first column  $[f_p(0), f_p(1), \dots, f_p(L_f - 1), [0]_{1 \times N-1}]^T$  and first row  $[f_p(0), [0]_{1 \times N-1}]$ ,  $[V_p]_{N \times Q_p}$  is the IFFT matrix that relevant to  $p^{\text{th}}$  sub-band carriers and  $\mathcal{S}_p$  is the column matrix of the  $p^{\text{th}}$  sub-band data sequence.

The received time-domain UPMC symbol after passing through the wireless channel has a length of  $L_h$  can be expressed as

$$y = \mathcal{H}X + z = \mathcal{H}\mathcal{F}\mathcal{V}\mathcal{S} + z \quad (5)$$

Where  $\mathcal{H}$  is the Toeplitz matrix of the channel coefficients  $h(n)$  with the first column  $[h(0), h(1), \dots, h(L_h - 1), [0]_{1 \times N+L_f-2}]^T$  and first row  $[h(0), [0]_{1 \times N+L_f-2}]$  and  $z$  is the zero mean Additive White Gaussian Noise (AWGN) vector having a length  $N_T = N + L - 2$ ;  $L = L_f + L_h$  with zero mean and variance of  $\sigma_z^2$ . At the receiver, unlike CP-OFDM, the UPMC uses the complete symbol duration of  $N_T$  samples. Therefore, the received UPMC symbol is padded with  $N - L + 2$  zeros for processing through 2N-point FFT. After execution of the 2N-point FFT, the even subcarriers extracted for data detection (down-sampled by a factor of 2) (explained appendix). Even subcarriers can be expressed as

$$Y_e = \mathcal{P}_e \mathcal{W} \mathcal{H} \mathcal{F} \mathcal{V} \mathcal{S} + \mathcal{P}_e^T \mathcal{W} z \quad (6)$$

Where the matrix  $[\mathcal{P}_e]_{N \times 2N}$  with elements

$$\mathcal{P}_e(m, k) = \begin{cases} 1; & \text{for } k = 2m \\ 0; & \text{for } k \neq 2m \end{cases} \quad (7)$$

Where  $m = 0, 1, \dots, N - 1$  and  $k = 0, 1, \dots, 2N - 1$

Where  $[\mathcal{W}]_{2N \times (N+L-2)}$  are the 2N-point FFT twiddle factor matrix and its elements are  $\mathcal{W}(k, r) = e^{-\frac{j2\pi}{2N}kr}$ ; where  $k = 0, 1, \dots, 2N - 1$ ; and  $r = 0, 1, \dots, N + L - 3$ . Now, these N frequency domain samples are used for data detection by the available knowledge from the OFDM system.

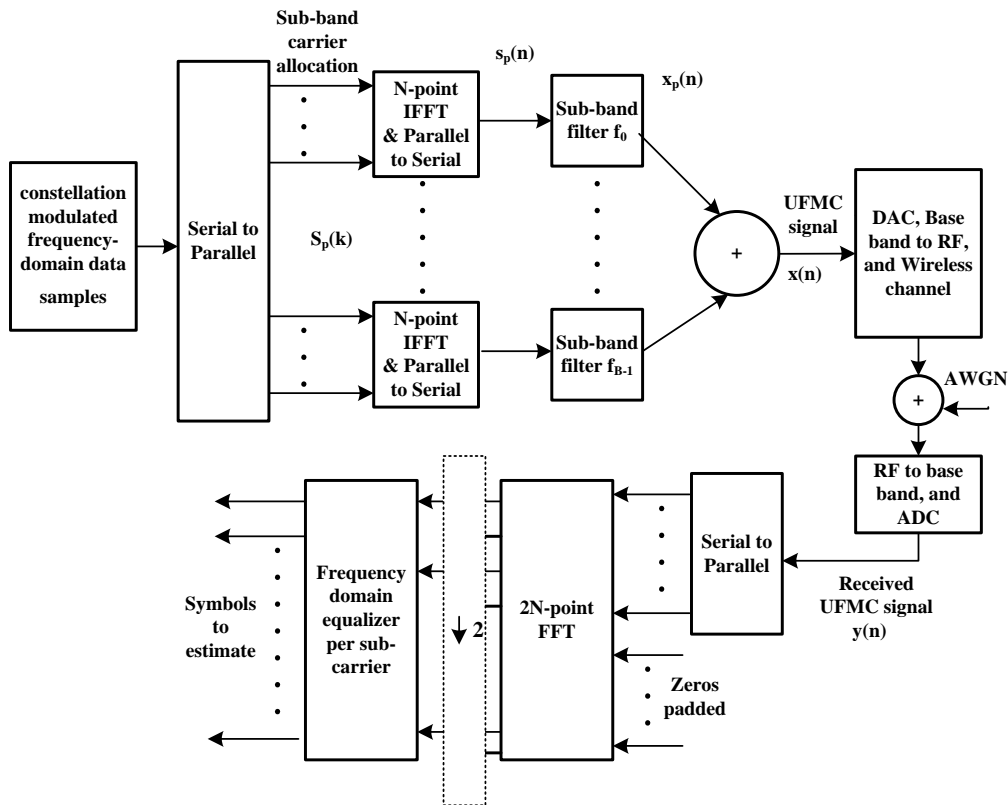


Figure 1. The UFMC system model

### 3 THE INTERFERENCE ANALYSIS IN UFMC SIGNAL

As we know that the FIR filtering operations provide less OBE and robustness in a relaxed synchronized system. But the filtering operation disrupts the orthogonality between the sub-carriers and causes interference. In general, the PRB based sub-band filtering is most preferable to implemented in the UFMC waveform [15]. In the case of multi-user and multi-services, there is design flexibility in the UFMC waveform to allocate multiple PRBs such that each service support multiple users, and one or more consecutive PRBs can be allocated to each user as shown in Figure 2. The inter-symbol interference (ISI) can be minimized by sub-band filtering operation in the UFMC system, but it might be causing some significant ISBI in the case of multi-service or multi-user systems as shown in figure 2. On the other hand the non-adjacent sub-bands/service bands/user bands, the ISBI is insignificant and does not affect the system performance.

#### 3.1 Closed-form for interference in the UFMC symbol

As stated earlier, the non-orthogonality due to filtering operation may introduce interference between the adjacent subcarriers and sub-bands. To analyze the interference, let us define the ISBI and ICI in terms of desired data symbols and sub-band filter metrics.

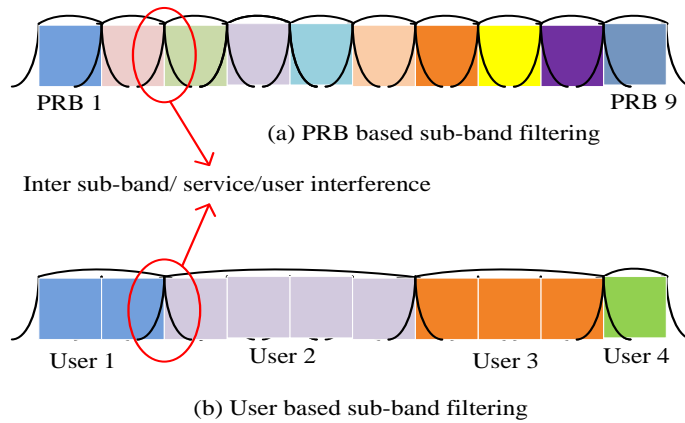


**Figure 2.** Types of sub-band filtering

Consider the following assumptions for formulation and simplification:

Assumption 1. The modulated data symbols mapping on subcarriers are uncorrelated with each other, have zero mean (i.e.,  $E[S_p(k)] = 0$  and variance  $E[|S_p(k)|^2] = \sigma_{s_p}^2$

Assumption 2. The sub-band filter coefficients are normalized to have  $\sum_{l=0}^{L-1} |f_p(l)|^2 = 1$

Consider the energy of the UPMC symbol given as

$$E_{UPMC} = \sum_{n=0}^{N+L-2} |x(n)|^2 = \sum_{n=0}^{N+L-2} x(n) x^*(n) \quad (8)$$

Proposition: The UPMC symbol energy consists of three components: the subcarrier energy ( $E_{sc}$ ), the interference between the subcarriers within the sub-band (ICI)  $E_{ICI}$ , and the interference between sub-bands in the symbol (ISBI)  $E_{ISBI}$ .

The energy of the UPMC symbol can be expressed as

$$E_{UPMC} = \sum_{n=0}^{N+L-2} \left( \sum_{p=0}^{B-1} x_p(n) \right) \left( \sum_{q=0}^{B-1} x_q^*(n) \right) = E_{SB} + E_{ISBI} \quad (9)$$

Where  $x^*(n)$  represents the complex conjugative of  $x(n)$ . By substituting (1) in (9), the UPMC symbol energy can be composed of two components, one is the total sub-band energy ( $E_{SB}$ ) for  $p = q$  and another one is the ISBI component ( $E_{ISBI}$ ) for  $p \neq q$ . These energy components can be expressed as

$$E_{SB} = \sum_{n=0}^{N+L-2} \sum_{p=q=0}^{B-1} |x_p(n)|^2 = \sum_{n=0}^{N+L-2} \sum_{p=0}^{B-1} \sum_{l=0}^{L-1} |f_p(l)|^2 R_{s_p, s_p} \quad (10)$$

$$E_{ISBI} = \sum_{n=0}^{N+L-2} \sum_{p=0}^{B-1} \sum_{\substack{q=0 \\ q \neq p}}^{B-1} x_p(n) x_q^*(n) = \sum_{n=0}^{N+L-2} \sum_{p=0}^{B-1} \sum_{\substack{q=0 \\ q \neq p}}^{B-1} \sum_{l=0}^{L-1} f_p(l) f_q^*(l) R_{s_p, s_q} \quad (11)$$

Where  $R_{s_p, s_q}$  is the correlation sequence of the two different time-domain sub-band data sequence  $s_p(n)$  and  $s_q(n)$ , which can be defined as  $R_{s_p, s_q} = s_p(n-l)s_q^*(n-l)$ . By substituting (3) here, we get

$$R_{s_p, s_q} = \frac{1}{N^2} \sum_{k=m=0}^{\min(Q_p, Q_q)} S_p(k)S_q^*(k) e^{j\frac{2\pi}{N}(K_p-K_q)(n-l)} + \frac{1}{N^2} \sum_{k=0}^{Q_p-1} \sum_{\substack{m=0 \\ m \neq k}}^{Q_q-1} S_p(k)S_q^*(m) e^{j\frac{2\pi}{N}(K_p-K_q+k-m)(n-l)} \quad (12)$$

$$R_{s_p, s_q} = \frac{1}{N^2} e^{j\frac{2\pi}{N}(K_p-K_q)(n-l)} \left( \sum_{k=0}^{\min(Q_p, Q_q)} S_p(k)S_q^*(k) + \sum_{k=0}^{Q_p-1} \sum_{\substack{m=0 \\ m \neq k}}^{Q_q-1} S_p(k)S_q^*(m) e^{j\frac{2\pi}{N}(k-m)(n-l)} \right) \quad (13)$$

Since the modulated data sequences (frequency-domain data sequences) are uncorrelated or low correlated for  $p \neq q$  and  $k \neq m$ . Therefore, neglecting the second term in (13) we have

$$R_{s_p, s_q} = \frac{1}{N^2} e^{j\frac{2\pi}{N}(K_p-K_q)(n-l)} \sum_{k=0}^{\min(Q_p, Q_q)} S_p(k)S_q^*(k) \quad (14)$$

For  $p = q$  the equation (13) can be written as

$$R_{s_p, s_p} = \frac{1}{N^2} \left( \sum_{k=0}^{Q_p-1} |S_p(k)|^2 + \sum_{k=0}^{Q_p-1} \sum_{\substack{m=0 \\ m \neq k}}^{Q_p-1} S_p(k)S_p^*(m) e^{j\frac{2\pi}{N}(k-m)(n-l)} \right) \quad (15)$$

From (2), we have

$$f_p(l)f_q^*(l) = |f(l)|^2 e^{j\frac{2\pi}{N}(K_p-K_q+\frac{Q_p-Q_q}{2})l} \quad (16)$$

Substitute (15) in (10), the total sub-band energy can be written as

$$E_{SB} = \sum_{n=0}^{N+L_f-2} \sum_{p=0}^{B-1} \sum_{l=0}^{L_f-1} |f_p(l)|^2 \frac{1}{N^2} \left( \sum_{k=0}^{Q_p-1} |S_p(k)|^2 + \sum_{k=0}^{Q_p-1} \sum_{\substack{m=0 \\ m \neq k}}^{Q_p-1} S_p(k)S_p^*(m) e^{j\frac{2\pi}{N}(k-m)(n-l)} \right) \quad (17)$$

According to (17), the total sub-band energy  $E_{SB}$  can be divided into two components: the sub-carrier energy ( $E_{SC}$ ) component for  $k = m$  and the ICI component ( $E_{ICI}$ ) for  $k \neq m$ . Therefore, the complete UPMC symbol energy becomes

$$E_{UPMC} = E_{SC} + E_{ICI} + E_{ISBI} \quad (18)$$

From Assumption 2 and  $N \gg L_f$ , the total desired data subcarriers energy of the UPMC symbol is given as

$$E_{SC} = \frac{1}{N^2} \sum_{n=0}^{N+L_f-2} \sum_{p=0}^{B-1} \sum_{l=0}^{L_f-1} |f_p(l)|^2 \sum_{k=0}^{Q_p-1} |S_p(k)|^2 = \frac{N+L_f-1}{N} \sum_{p=0}^{B-1} \sum_{k=0}^{Q_p-1} |S_p(k)|^2 \quad (19)$$

and

$$E_{ICI} = \frac{1}{N^2} \sum_{p=0}^{B-1} \sum_{k=0}^{Q_p-1} \sum_{\substack{m=0 \\ m \neq k}}^{Q_q-1} S_p(k) S_p^*(m) \sum_{n=0}^{N+L_f-2} e^{j\frac{2\pi}{N}(k-m)n} E_{f_p}(k, m) \quad (20)$$

Where

$$E_{f_p}(k, m) = \sum_{l=0}^{L-1} |f_p(l)|^2 e^{-j\frac{2\pi}{N}((k-m)l)} \quad (21)$$

Substituting (14) and (16) in (11), the inter sub-band interference energy can be written as

$$E_{ISBI} = \frac{1}{N^2} \sum_{p=0}^{B-1} \sum_{\substack{q=0 \\ q \neq p}}^{B-1} \sum_{l=0}^{L-1} |f(l)|^2 e^{-j\frac{2\pi}{N}(\frac{Q_p-Q_q}{2})l} \sum_{n=0}^{N+L_f-2} e^{j\frac{2\pi}{N}(k_p-k_q)n} \sum_{k=0}^{\min(Q_p, Q_q)} S_p(k) S_q^*(k) \quad (22)$$

### 3.2 Interference analysis in the UFMC symbol

According to (20) and (22), both ICI and ISBI depend on the sub-band filter ramps on both sides of the sub-band and the size of the sub-band. The filter ramps depend on the filter length, which is usually recommended to choose more than the channel length (CP length) to mitigate the multipath channel dispersion. Therefore, the filter length impacts the performance in different ways based on the sub-band size and the maximum-to-minimum filter gain ratio (MMFGR) among the subcarriers within a particular sub-band. To demonstrate this, consider different cases as shown in Figure 3, the sub-band ramps (i.e., OBE) due to filtering operation extended to more than one sub-band for smaller sub-band size ( $Q_p$ ) and the ramp spread is less than the one adjacent sub-band with fixed filter length. Thus, the ISBI due to adjacent sub-band is more in case of smaller sub-band widths than the larger sub-band widths.

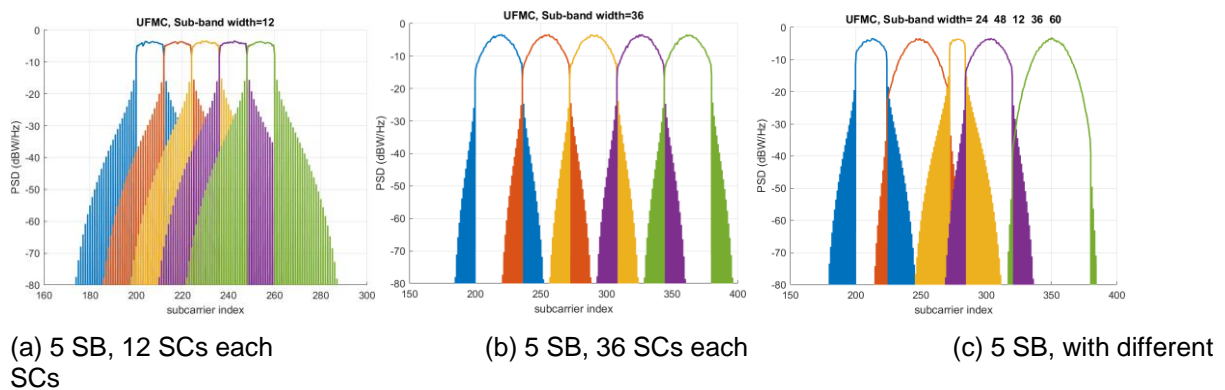


**Figure 3** Power spectral density of the UFMC signal with the following specifications: filter length ( $L_f$ ) = 73 and  $N = 1024$ .

In addition, shorter filter length or narrow sub-band width leads to bad frequency localization, and low MMFGR (i.e., the power allocation among the subcarriers in a

sub-band is uniform) as shown in Figure 4. and thus, smaller performance loss. The UPMC system with a longer filter length results in a larger MMFGR (i.e., non-uniform power allocation among the subcarrier within a sub-band and higher at the middle of the sub-band) and higher frequency selectivity, but it leads to a high possibility of error at the edges of the sub-band and causes a greater overall performance loss.

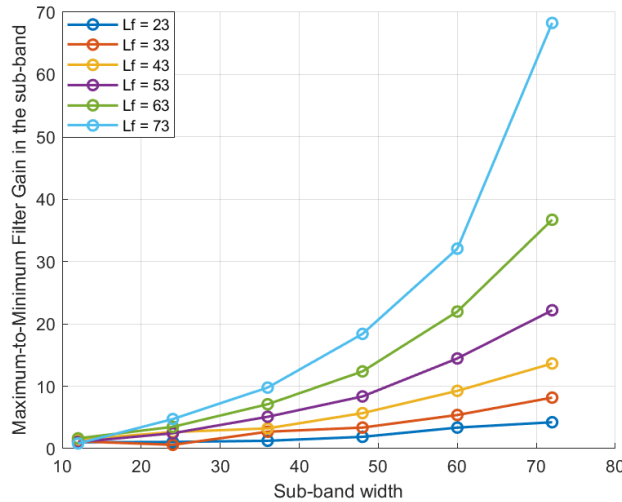


Figure 4 MMFGR variation according to the filter length and sub-band width

### 3.3 Optimal filter length configuration for sub-band filter

The sub-band filter design flexibility is one of the most significant advantages of the UPMC waveform compared to others, which enables to adjustment of the sub-band filtering configuration according to the requirement of service, user, and channel conditions. According to Gibb's phenomenon, the magnitude response of the filter gives almost the same oscillatory behavior (i.e., ripples) after a finite value of its order. From this perspective point of view, we proposed a method that adopted the FIR filter order with respective sub-band sizes for flexible symbol duration and hence latency by maintaining a minimum level of OBE. In general, the filter design algorithms have been developed by a tolerance scheme, for an approximation to the ideal filter frequency response. The FIR filter design depends on the following parameters: passband ( $f_p$ ) and stopband edge frequencies ( $f_s$ ), maximum absolute errors known as ripples in the passband and stopband ( $\delta_p$  and  $\delta_s$ ) and filter length (L).

The sub-band filter length (L) is defined approximately as [22]

$$L = \frac{-10 \log(\delta_p \delta_s) - 13}{14.36 \Delta f} \quad (23)$$

Where  $\Delta f$  represents the normalized transition width, which is defined as the difference between stopband edge frequency and passband edge frequency i.e.,  $\Delta f = \frac{(f_s - f_p)}{F_s}$ . The passband and stopband edge frequencies can be defined based on the bandwidth requirements of the sub-band/ service. The bandwidth (BW) of the filter is defined from the number of subcarriers allocated to the sub-band as  $BW = Q f_{sc}$ , where  $f_{sc}$  is the subcarrier spacing, typically an integer multiple of 15

kHz for NR numerology. The lower ( $f_l$ ) and upper ( $f_h$ ) passband edge frequencies of the sub-band are defined as

$$f_l = K_0 f_{sc} \text{ and } f_h = (K_0 + Q_p) f_{sc} \quad (24)$$

Here the stopband frequency is determined from the general filter assumption, i.e., half of the sampling frequency  $\frac{F_s}{2}$  or the guard band between the sub-band or service bands i.e.,  $f_s = \frac{N}{2} f_{sc}$  and  $\Delta f = \frac{1}{2} - \frac{K_0 + Q_p}{N}$ . Substitute  $\Delta f$  in (23), we get

$$L = \frac{N(-10 \log(\delta_p \delta_s) - 13)}{7.18(N - K_0 - Q_p)} \quad (25)$$

The sub-band filter length decides the level of non-orthogonality factor between subcarriers, the OBE, and hence the interference (ISBI and ICI). In this paper, the sub-band FIR filter length is adapted with respect to the sub-band size as mentioned in (25) to maintain a minimum level of interference. That is the filter length or tail in the symbol duration due to filtering operation can be flexible based on the sub-band width.

#### 4. SIMULATION RESULTS

From the early discussion, the system performance is affected by the sub-band filter design for a given width of the sub-band. The longer filter length leads to lower OBE in the adjacent sub-band (only some edge subcarriers may suffer from OBE), but the out of band radiation extends to a greater number of sub-bands with insignificant value within a sub-band. However, the cumulative ISBI increases with the number of sub-bands, and the ICI may increase with filter length due to a higher level of non-orthogonality. On other hand, the short filter length reduces overhead, lesser frequency localization, spreads higher OBE into more than one adjacent sub-bands but is limited to some sub-bands within the symbol resulting in more ISBI on the immediate adjacent sub-band as shown in Figure 5. To investigate the level of ISBI and ICI within the UFMC symbol we consider three cases for bandwidth of 10 MHz, 15 kHz subcarrier spacing, and the FFT size of 1024 as shown in Figure 6. In the case of uniform sub-band allocation, when the sub-band has a width of 12 SCs as shown in Figure 6(a) both ISBI and ICI increase with filter length. The ISBI decreases and ICI increase with the filter length for a larger size of the sub-band as shown in Figure 6(b). Thus, there is a tradeoff between the interference and the sub-band width i.e., the dominated interference (ISBI) increases for narrow sub-band and decreases for wide sub-band.

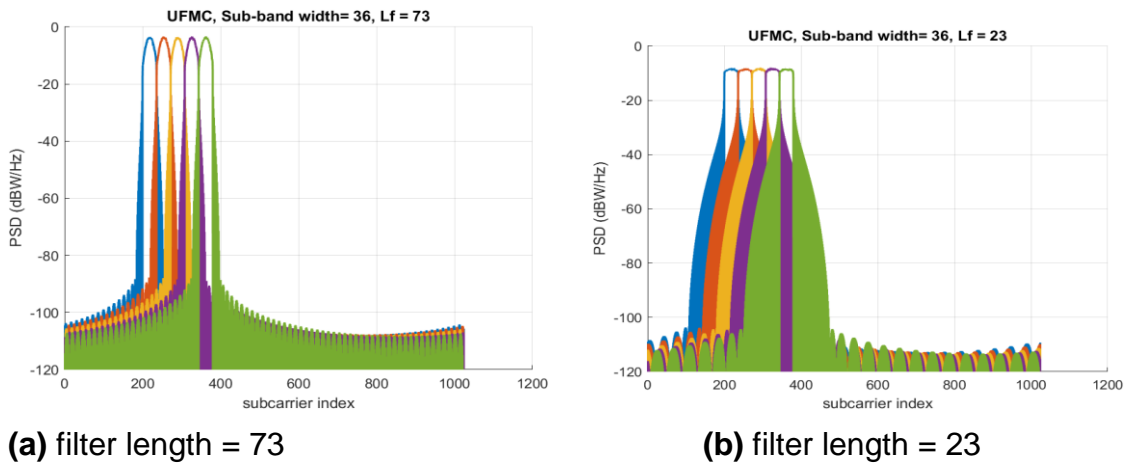


**Figure 5** Power spectral density spread within the UFMC symbol

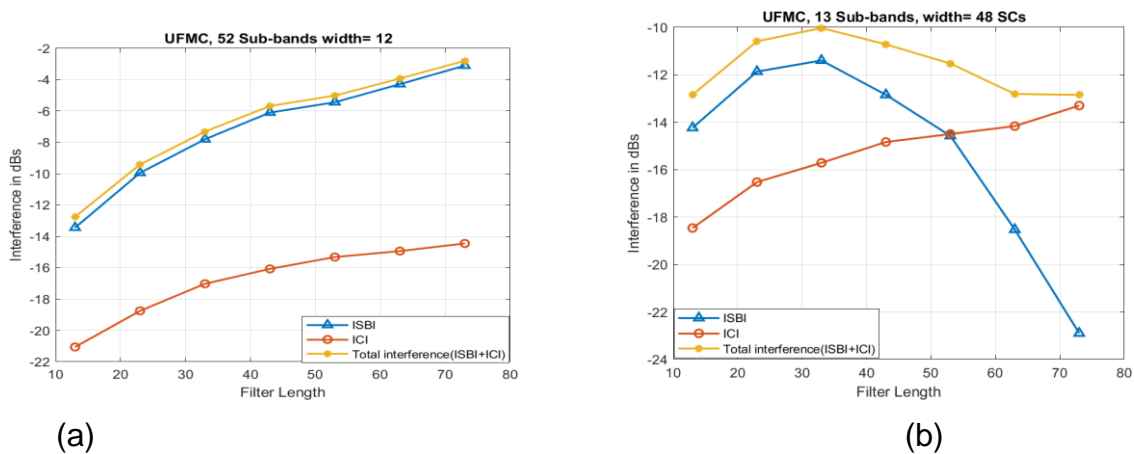


**Figure 6** Interference variation in the UFMC symbol for uniform sub-band allocation  
 (a)  $Q = 12$  SCs (b)  $Q = 48$  SCs

To reduce this effect the sub-band filter length can be dynamically modified with sub-band size to minimize the overall interference in the UFMC symbol. The simulation results as shown in Figure 7, demonstrate the variation of average ISBI and ICI per sub-band for bandwidth of 10 MHz, sub-carrier spacing of 15 kHz with sub-band sizes 12, 36, 48, 72, and 96. From this, we concluded that the proposed model is superior in terms of ISBI compared to the conventional UFMC system and the ICI component increases with sub-band size and which is more for lower sub-band sizes.

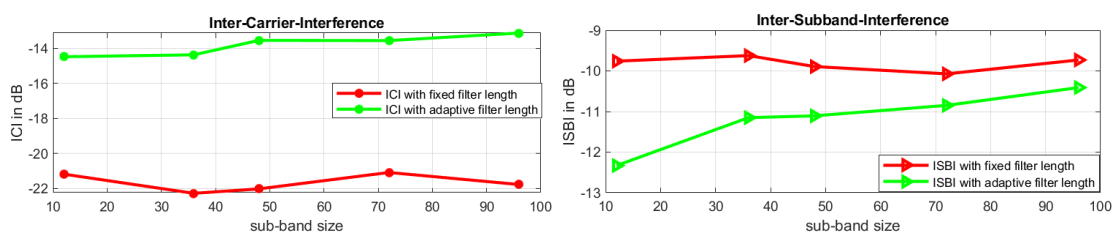


**Figure 7** ISBI and ICI variation with sub-band size

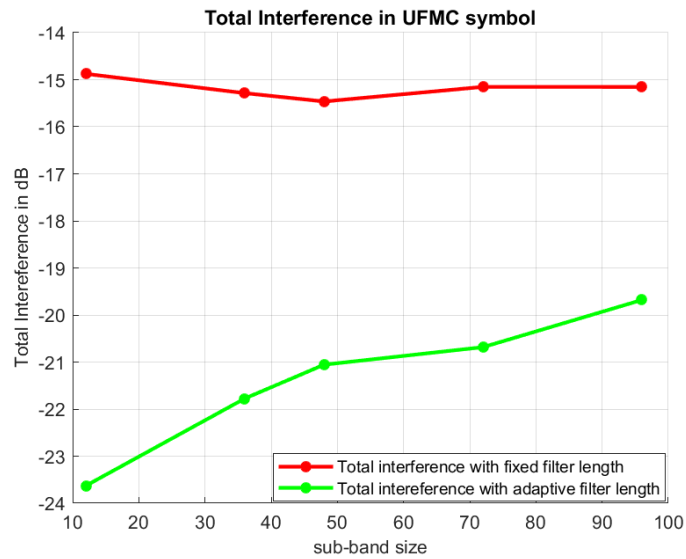


**Figure 8** Total interference versus sub-band size

With the proposed design of the adaptive filter approach, the total interference (ICI+ISBI) is reduced by around 8 to 9 dB as shown in Figure 8. Furthermore, the proposed approach gives a better signal to interference ratio (SIR) compared to the conventional one as shown in Figure 9. In addition, it reduces the symbol overhead due to the filter tail and leads to the smaller frequency selectivity of the sub-band (i.e., lesser frequency localization). Thus, the proposed approach is most suitable for enhanced broadband and URLLC services.

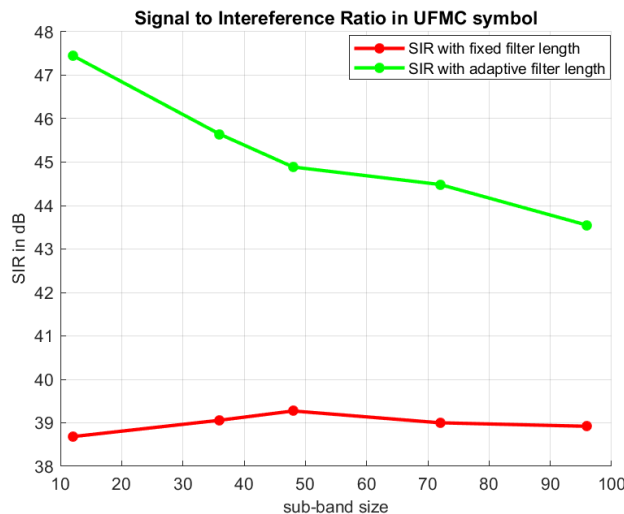


**Figure 9** Signal to Interference Ratio versus sub-band size

## 5. CONCLUSIONS

The UFMC is one of the emerging waveform technologies for next-generation wireless networks because of its abilities. Due to the filtering operation in the UFMC system, the orthogonality destroyed between the subcarriers and hence generates interference. In this article, the interference was analyzed in the UFMC symbol by deriving the closed form of the interference energy related to the sub-band filter impulse response. According to the analysis, the generated ISBI is significantly more and the ICI is less for the narrow sub-bands, and for wide sub-band, the ISBI is less and the ICI increases with filter length. In addition, the filter length was dynamically modified to minimize interference. This approach reduces the interference by approximately 8 to 9 dBs thus improving the system performance.

## REFERENCES

- [1] L. U. Khan, I. Yaqoob, M. Imran, Z. Han, and C. S. Hong, "6G Wireless Systems: A Vision, Architectural Elements, and Future Directions," *IEEE Access*, vol. 8, pp. 147029–147044, 2020, doi: 10.1109/ACCESS.2020.3015289.
- [2] W. Saad, M. Bennis, and M. Chen, "A Vision of 6G Wireless Systems: Applications, Trends, Technologies, and Open Research Problems," *IEEE Netw.*, vol. 34, no. 3, pp. 134–142, 2020, doi: 10.1109/MNET.001.1900287.
- [3] M. Alsabah *et al.*, "6G Wireless Communications Networks: A Comprehensive Survey," *IEEE Access*, vol. 9, pp. 148191–148243, 2021, doi: 10.1109/ACCESS.2021.3124812.
- [4] H. Sampath, S. Talwar, J. Tellado, V. Erceg, and A. Paulraj, "A fourth-generation MIMO-OFDM broadband wireless system: design, performance, and field trial results," *IEEE Commun. Mag.*, vol. 40, no. 9, pp. 143–149, 2002, doi: 10.1109/MCOM.2002.1031841.
- [5] P. Banelli, S. Buzzi, G. Colavolpe, A. Modenini, F. Rusek, and A. Ugolini, "Modulation Formats and Waveforms for 5G Networks: Who Will Be the Heir of OFDM?: An overview of alternative modulation schemes for improved spectral efficiency," *IEEE Signal Process. Mag.*, vol. 31, no. 6, pp. 80–93, 2014, doi: 10.1109/MSP.2014.2337391.
- [6] M. Elkourdi, B. Peköz, E. Güvenkaya, and H. Arslan, "Waveform design principles for 5G and beyond," in *2016 IEEE 17th Annual Wireless and Microwave Technology Conference (WAMICON)*, 2016, pp. 1–6, doi: 10.1109/WAMICON.2016.7483859.
- [7] A. A. Zaidi *et al.*, "Waveform and Numerology to Support 5G Services and Requirements," *IEEE Commun. Mag.*, vol. 54, no. 11, pp. 90–98, 2016, doi: 10.1109/MCOM.2016.1600336CM.
- [8] G. Fettweis, M. Krondorf, and S. Bittner, "GFDM - Generalized Frequency Division Multiplexing," in *VTC Spring 2009 - IEEE 69th Vehicular Technology Conference*, 2009, pp. 1–4, doi: 10.1109/VETECS.2009.5073571.
- [9] R. Nissel, S. Schwarz, and M. Rupp, "Filter Bank Multicarrier Modulation Schemes for Future Mobile Communications," *IEEE J. Sel. Areas Commun.*, vol. 35, no. 8, pp. 1768–1782, 2017, doi: 10.1109/JSAC.2017.2710022.
- [10] L. Zhang, A. Ijaz, P. Xiao, M. M. Molu, and R. Tafazolli, "Filtered OFDM Systems, Algorithms, and Performance Analysis for 5G and Beyond," *IEEE Trans. Commun.*, vol. 66, no. 3, pp. 1205–1218, 2018, doi: 10.1109/TCOMM.2017.2771242.
- [11] V. Vakilian, T. Wild, F. Schaich, S. ten Brink, and J. Frigon, "Universal-filtered multi-carrier technique for wireless systems beyond LTE," in *2013 IEEE Globecom Workshops (GC Wkshps)*, 2013, pp. 223–228, doi: 10.1109/GLOCOMW.2013.6824990.

- [12] F. Schaich and T. Wild, "Waveform contenders for 5G — OFDM vs. FBMC vs. UFMC," in *2014 6th International Symposium on Communications, Control and Signal Processing (ISCCSP)*, 2014, pp. 457–460, doi: 10.1109/ISCCSP.2014.6877912.
- [13] F. Schaich, T. Wild, and Y. Chen, "Waveform Contenders for 5G - Suitability for Short Packet and Low Latency Transmissions," in *2014 IEEE 79th Vehicular Technology Conference (VTC Spring)*, 2014, pp. 1–5, doi: 10.1109/VTCSpring.2014.7023145.
- [14] S. Wei, H. Li, W. Zhang, and W. Cheng, "A Comprehensive Performance Evaluation of Universal Filtered Multi-Carrier Technique," *IEEE Access*, vol. 7, pp. 81429–81440, 2019, doi: 10.1109/ACCESS.2019.2923774.
- [15] L. Zhang, A. Ijaz, P. Xiao, and R. Tafazolli, "Multi-Service System: An Enabler of Flexible 5G Air Interface," *IEEE Commun. Mag.*, vol. 55, no. 10, pp. 152–159, 2017, doi: 10.1109/MCOM.2017.1600916.
- [16] L. Zhang, A. Ijaz, P. Xiao, A. Quddus, and R. Tafazolli, "Subband Filtered Multi-Carrier Systems for Multi-Service Wireless Communications," *IEEE Trans. Wirel. Commun.*, vol. 16, no. 3, pp. 1893–1907, 2017, doi: 10.1109/TWC.2017.2656904.
- [17] M. Mukherjee, L. Shu, V. Kumar, P. Kumar, and R. Matam, "Reduced out-of-band radiation-based filter optimization for UFMC systems in 5G," in *2015 International Wireless Communications and Mobile Computing Conference (IWCMC)*, 2015, pp. 1150–1155, doi: 10.1109/IWCMC.2015.7289245.
- [18] X. Wang, T. Wild, and F. Schaich, "Filter Optimization for Carrier-Frequency- and Timing-Offset in Universal Filtered Multi-Carrier Systems," in *2015 IEEE 81st Vehicular Technology Conference (VTC Spring)*, 2015, pp. 1–6, doi: 10.1109/VTCSpring.2015.7145842.
- [19] Z. Zhang, H. Wang, G. Yu, Y. Zhang, and X. Wang, "Universal Filtered Multi-Carrier Transmission With Adaptive Active Interference Cancellation," *IEEE Trans. Commun.*, vol. 65, no. 6, pp. 2554–2567, 2017, doi: 10.1109/TCOMM.2017.2681668.
- [20] X. Chen, L. Wu, Z. Zhang, J. Dang, and J. Wang, "Adaptive Modulation and Filter Configuration in Universal Filtered Multi-Carrier Systems," *IEEE Trans. Wirel. Commun.*, vol. 17, no. 3, pp. 1869–1881, 2018, doi: 10.1109/TWC.2017.2786231.
- [21] L. Zhang, A. Ijaz, P. Xiao, K. Wang, D. Qiao, and M. A. Imran, "Optimal Filter Length and Zero Padding Length Design for Universal Filtered Multi-Carrier (UFMC) System," *IEEE Access*, vol. 7, pp. 21687–21701, 2019, doi: 10.1109/ACCESS.2019.2898322.
- [22] L. R. Rabiner, J. H. McClellan, and T. W. Parks, "FIR digital filter design techniques using weighted Chebyshev approximation," *Proc. IEEE*, vol. 63, no. 4, pp. 595–610, 1975, doi: 10.1109/PROC.1975.9794.